



Article

Development of the Chinese Space-Based Radiometric Benchmark Mission LIBRA

Peng Zhang ^{1,2}, Naimeng Lu ^{1,2}, Chuanrong Li ^{3,*}, Lei Ding ⁴, Xiaobing Zheng ⁵, Xuejun Zhang ⁶, Xiuqing Hu ^{1,2}, Xin Ye ⁶, Lingling Ma ³, Na Xu ^{1,2}, Lin Chen ^{1,2} and Johannes Schmetz ⁷

- ¹ Key Laboratory of Radiometric Calibration and Validation for Environmental Satellite, China Meteorological Administration, Beijing 100081, China; zhangp@cma.gov.cn (P.Z.); lunm@cma.gov.cn (N.L.); huxq@cma.gov.cn (X.H.); xuna@cma.gov.cn (N.X.); chenlin@cma.gov.cn (L.C.)
- ² National Satellite Meteorological Center, China Meteorological Administration, Beijing 100081, China
- ³ Aerospace Information Research Institute, Chinese Academy of Sciences, Beijing 100094, China; llma@aoe.ac.cn
- ⁴ Shanghai Institute of Technical Physics, Chinese Academy of Sciences, Shanghai 200083, China; leiding@mail.sitp.ac.cn
- ⁵ Anhui Institute of Optics and Fine Mechanics, Chinese Academy of Sciences, Hefei 230031, China; xbzheng@aiofm.ac.cn
- ⁶ Changchun Institute of Optics, Fine Mechanics and Physics, Chinese Academy of Sciences, Changchun 130033, China; zxj@ciomp.ac.cn (X.Z.); yexin@ciomp.ac.cn (X.Y.)
- ⁷ Retired former Chief Scientist of Eumetsat, Eumetsat Allee 1, D-64295 Darmstadt, Germany; johannesschmetz@gmail.com
- * Correspondence: crli@aoe.ac.cn; Tel.: +86-13701390352

Received: 26 May 2020; Accepted: 6 July 2020; Published: 8 July 2020



Abstract: Climate observations and their applications require measurements with high stability and low uncertainty in order to detect and assess climate variability and trends. The difficulty with space-based observations is that it is generally not possible to trace them to standard calibration references when in orbit. In order to overcome this problem, it has been proposed to deploy space-based radiometric reference systems which intercalibrate measurements from multiple satellite platforms. Such reference systems have been strongly recommended by international expert teams. This paper describes the Chinese Space-based Radiometric Benchmark (CSRB) project which has been under development since 2014. The goal of CSRB is to launch a reference-type satellite named LIBRA in around 2025. We present the roadmap for CSRB as well as requirements and specifications for LIBRA. Key technologies of the system include miniature phase-change cells providing fixed-temperature points, a cryogenic absolute radiometer, and a spontaneous parametric down-conversion detector. LIBRA will offer measurements with SI traceability for the outgoing radiation from the Earth and the incoming radiation from the Sun with high spectral resolution. The system will be realized with four payloads, i.e., the Infrared Spectrometer (IRS), the Earth-Moon Imaging Spectrometer (EMIS), the Total Solar Irradiance (TSI), and the Solar spectral Irradiance Traceable to Quantum benchmark (SITQ). An on-orbit mode for radiometric calibration traceability and a balloon-based demonstration system for LIBRA are introduced as well in the last part of this paper. As a complementary project to the Climate Absolute Radiance and Refractivity Observatory (CLARREO) and the Traceable Radiometry Underpinning Terrestrial- and Helio- Studies (TRUTHS), LIBRA is expected to join the Earth observation satellite constellation and intends to contribute to space-based climate studies via publicly available data.

Keywords: earth observation; climate observation; radiometric metrology; calibration benchmark; SI traceability

1. Introduction

The role of satellites in Earth observation has increased substantially over the past sixty years since the first meteorological satellite TIROS 1 was launched in 1960. With satellite observations, we are able to probe the Earth system (atmosphere, ocean, and land surface) at increasingly high temporal, spatial, and spectral resolution [1]. However, the capability for climate monitoring from space is insufficient [2–4]. Even though satellite observed radiances today generally have a radiometric precision of 0.2 K or better, radiances assimilated in numerical weather prediction (NWP) models still need to be corrected for significant biases. For climate monitoring, current measurements are not yet adequate because small trends of the order of a tenth of a degree need to be measured with high confidence [5,6]. It is essential for climate monitoring and desirable for NWP that measurements are basically bias-free [7].

Without accurate, high quality observations on relevant time and space scales, climate science applications and services will be limited [8]. To anchor satellite-based climate observation, several reference-type missions against an absolute standard are being considered by several space agencies [9]. The Traceable Radiometry Underpinning Terrestrial- and Helio-Studies (TRUTHS [10] has been accepted by the ESA (European Space Agency) as a climate mission with an unprecedented SI-traceable accuracy. The Climate Absolute Radiance and Refractivity Observatory (CLARREO) mission has been underway by the National Aeronautics and Space Administration (NASA) since the mid-2000s. CLARREO also aims to provide accurate and SI-traceable observations, allowing the assessment of decadal changes of climate [11]. More recently, a CLARREO Pathfinder mission with only the reflected solar spectrometer is being built for the International Space Station (ISS), with launch tentatively planned for 2023.

The proposed CLARREO and TRUTHS missions would create a climate observing system measuring both the incoming and reflected solar energy with a 10-fold increase in data accuracy compared to existing systems. They would provide spectrally resolved thermal infrared and reflected solar radiation with high absolute accuracy. In addition, such systems will serve as on-orbit references for a wide range of visible and infrared Earth observation sensors in LEO and GEO orbits. This approach has already been realized by the Global Space-based Intercalibration System (GSICS) using the most stable current instruments as references [12].

In the recent Vision 2040 document of the WMO Integrated Observing System (WIGOS), it is presumed that operational meteorological satellite systems will remain the key elements of a space-based climate observing system capable of unambiguously monitoring indicators of changes in the Earth's climate [13]. Satellite agencies are therefore encouraged to develop new satellite instruments with climate applications in mind. The proposed reference systems would go a long way in that direction. This will also enable the production of much improved Essential Climate Variables (ECVs) in accordance with established key requirements for climate monitoring [14].

Realizing the importance of reference-type missions for improving climate science and for harmonizing global satellite observations, an expert team on Earth observation and navigation of Ministry of Science and Technology (MOST) proposed the concept of the Chinese Space-based Radiometric Benchmark (CSRB) in 2006. The CSRB project was approved and initially funded by MOST in 2014. To date, Phase A of the CSRB project, completed in 2018, resolved the fundamental problems of building the SI-traceable calibrator for the thermal infrared band and reflected solar band. The ultimate goal of the CSRB project is to build a flight model of the Chinese radiometric benchmark satellite, named 'LIBRA', for launch during 2022–2025. The roadmap of the CSRB project is presented in Section 2, and the requirements and specifications for LIBRA follow in Section 3. The payloads and key technologies are briefly described in Section 4. The on-orbit operations for radiometric calibration traceability and the balloon-based demonstration experiments are introduced in Sections 5 and 6, respectively.

2. CSRB Project in China

China has established a comprehensive constellation network for space-based Earth observations with a perspective over 50 years. Currently, there are multiple satellite series operating in orbit, including the Fengyun (FY) meteorological satellites since 1988, the Ziyuan (ZY) Earth resources satellites since 1999, the Haiyang (HY) ocean satellites since 2002, and the Huanjing (HJ) environment and disaster monitoring satellites since 2008. More recently, a new Earth observation system with high spatial, temporal, and spectral resolution, named ‘Gaofeng’ (GF), was developed and has operated since 2013, achieving all-weather, all-day, and global coverage observation capability and providing operational applications and services in the fields of agriculture, disaster, resource, and environmental studies [15].

In the early stages of China’s Earth observation satellite programs, there were hardly any onboard calibration systems. On-orbit radiometric accuracy was estimated by pre-launch calibrations and later corrected by vicarious calibrations using the Chinese Radiometric Calibration Site (CRCS) in the Dunhuang Gobi Desert for reflected solar bands and Qinghai Lake for thermal infrared bands [16]. Onboard calibration systems were realized with the advent of the second generation Fengyun polar orbiting meteorological satellite (FY-3A) in the middle of the 2000s [17]. Best practice guidelines for pre-launch characterization and calibration for passive optical remote sensing instruments are strictly followed to achieve adequate absolute accuracy and stability of the instruments in orbit [18–20]. To provide a space-based radiometric reference for Earth observations from multiple satellite platforms and in order to respond to requirements by the Global Climate Observing System (GCOS), the CSRB concept was proposed by an expert team on Earth observation and navigation of the Ministry of Science and Technology in 2006 [21]. The project has three phases: Phase A, extended from 2014 to 2018, with the goal to develop the SI-traceable calibrator for the thermal infrared band (IR) and the reflective solar band (RSB). Phase B, from 2018 to 2022, has the objective to develop an engineering model of the reference instruments. During Phase C, from 2022 to 2025, a flight model ready for launch will be developed. The roadmap of the CSRB project is shown in Figure 1.

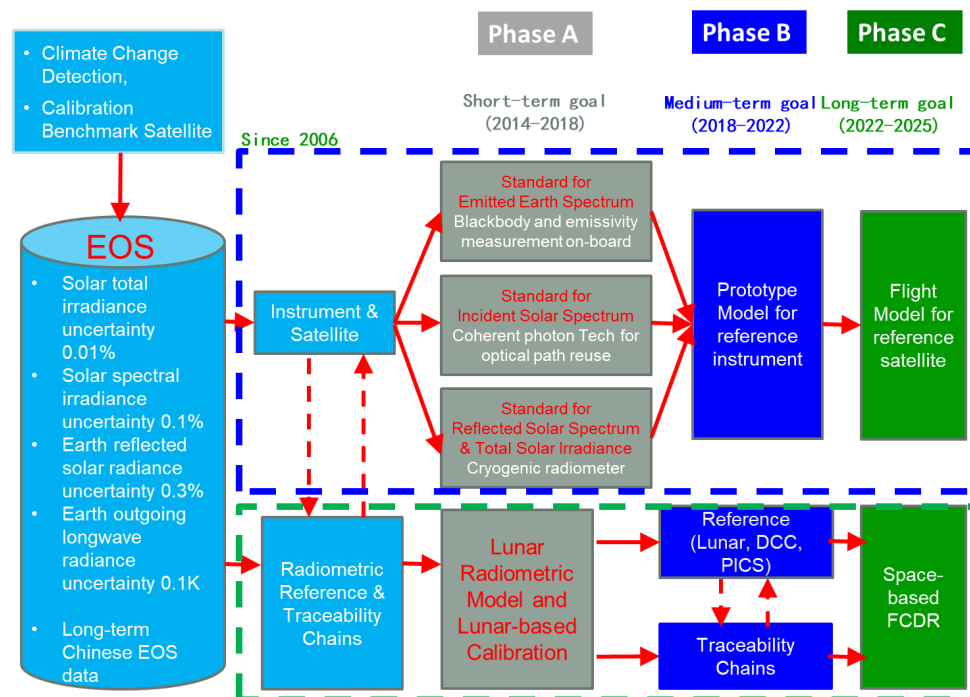


Figure 1. The roadmap of the Chinese Space-based Radiometric Benchmark (CSRB) project. EOS is the acronym for Earth Observation System, DCC for Deep Convective Cloud, PICS for Pseudo Invariant Calibration Sites, and FCDR for Fundamental Climate Data Record.

To date, Phase A has been completed. The prototypes, including an absolute radiance standard IR calibrator based on ITS-90 miniature phase-change temperature points, a RSB self-correction absolute calibrator based on Spontaneous Parametric Down-Conversion (SPDC) principles with eight spectral bands spanning 450–1000 nm, and a cavity-type absolute cryogenic radiometer (ACR) with 20 K operational temperature, were built together with the corresponding radiometric scale transfer chains. In this exploratory phase, an uncertainty better than 0.15 K and 0.3% was achieved for all of the three benchmark calibrators. Based on these promising results, Phase B of the CSRB project was started in 2018 and the engineering model is ongoing.

3. Prototype Model of LIBRA

3.1. Specification of LIBRA

The LIBRA mission consists of one satellite carrying four payloads: an Infrared Spectrometer (IRS) with hyperspectral resolution, an Earth-Moon Imaging Spectrometer (EMIS) measuring in reflected solar radiation, a Total Solar Irradiance (TSI) instrument, and a Solar spectral Irradiance monitoring instrument Traceable to Quantum benchmark (SITQ). A GPS/Beidou Global Navigation Satellite System Radio Occultation (GPS/BD GNSS RO) will be an optional instrument depending on the spacecraft bus capability. The detailed payload specifications of the LIBRA prototype model and the key technologies used are listed in Table 1. The IRS will be positioned on the spacecraft bus deck for nominal nadir views. Using an internal mirror, the IRS will enable nadir, off-nadir, internal calibration, and deep-space (zenith) observations. The EMIS and TSI will be co-boresighted and mounted to a two-axis gimbal to enable nadir (nominal operations) and off-nadir lunar and solar observations. The spacecraft bus should provide an independent means for acquiring necessary position and attitude information.

Table 1. Detailed payloads specifications of the LIBRA prototype model.

Instrument Name	Payload Requirements	Key Technology
IRS	Spectral range: 600–2700 cm ⁻¹ Spectral resolution: 0.5 cm ⁻¹ IFOV: 24 mrad Sensitivity: 0.1 K@270 K Emissivity of BB: ≥0.999 Measurement uncertainty: 0.15 K (k = 2)	Miniature fixed-temperature phase-change cells
EMIS	Spectral range: 380–2350 nm, Spectral resolution: 10 nm, Spectral precision: 0.5 nm, Spatial resolution: 100 m, Coverage: 50 km, Measurement uncertainty: 1% (k = 2)	Space Cryogenic Absolute Radiometer
TSI	Spectral range: 0.2–35 μm, Measurement uncertainty: 0.05% (k = 2) Long-term stability: 0.005%	Space Cryogenic Absolute Radiometer
SITQ	Spectral range: 380–2500 nm, Spectral resolution: 3 nm (380–1000 nm), 8 nm (1000–2500 nm) Spectral precision: 0.1–0.3 nm, Self-calibration uncertainty: 0.2%, Measurement uncertainty: 0.35% (k = 2)	Spontaneous Parametric Down-Conversion

The LIBRA experimental observatory has been designed for an operational lifetime of five years with consumables for eight years. The follow-up operational satellites will be designed for a long-term mission (20 years or more), with satellites in orbit overlapping in time. The spacecraft operations system will be designed to minimize the cost and risk of operations, including minimizing the number

of operators required to safely command and control the spacecraft, and maximizing use of spacecraft and ground system fault detection, reporting and protection tools.

Other potential platforms considered for the LIBRA mission include the Chinese Space Station (CSS) as an instrument platform and independent small satellite missions with only one SI instrument each. Lagrangian orbit locations are also being investigated for complementary observations.

3.2. Comparison with CLARREO and TRUTHS

As space-based climate and calibration observatories, the proposed CLARREO and TRUTHS missions have important potential contributions to make both directly through well-calibrated measurements and indirectly through facilitating intercalibration of the data from other platforms. By using advanced technologies, such as phase-change points, a cryogenic absolute radiometer, and spontaneous parametric down-conversion (SPDC), LIBRA will provide measurements with SI traceability for both the IR and the reflected solar components. The main characteristics of LIBRA, CLARREO, and TRUTHS are summarized in Table 2. More details of the LIBRA technologies will be introduced in the next section.

Table 2. Comparison among radiometric benchmark satellite.

Satellite	Libra				Clarreo			Truths	
Instrument Type *	IR	RS	TS	SS	IR	RS	RS	TS	SS
Spectral Coverage	600–2700 cm ⁻¹	380–2350 nm	0.2–35 µm	380–2500 nm	200–2000 cm ⁻¹	320–2300 nm	380–2300 nm	0.2–35 µm	320–2450 nm
Spectral Resolution	0.5 cm ⁻¹	10 nm	–	3–8 nm	0.5 cm ⁻¹	8 nm	5–10 nm	–	1–10 nm
Measurement Uncertainty	0.15 K (k = 2)	1% (k = 2)	0.05% (k = 2)	0.35% (k = 2)	0.065 K (k = 2)	0.3% (k = 2)	0.1% (k = 2)	0.02% (k = 2)	0.2% (k = 2)
SI-traceability	Yes	Yes	Yes	Yes	Yes	Yes	Yes	Yes	Yes

* In the line ‘Instrument type’, IR represents the instrument to measure the spectrally resolved infrared radiance, RS represents the instrument to measure the spectrally resolved reflectance of solar radiation, TS represents the instrument to measure the total solar irradiance, and SS represents the instrument to measure the spectrally resolved solar irradiance.

4. Instrument Design and Key Technologies

4.1. EMIS and TSI Make Use of the Space Cryogenic Absolute Radiometer (SCAR)

In order to improve the measurement accuracy and long-term stability of the reflective solar band and the total solar irradiance observations, it is important to develop a new onboard calibration system with high accuracy. The LIBRA will provide a calibrated reflected solar spectrum and total solar irradiance based on the Space Cryogenic Absolute Radiometer (SCAR) [22], instead of a solar diffuser, standard lamps, vicarious calibration methods, and ground-based calibration techniques. The prototype payload under development since 2018 is illustrated in Figure 2. Essentially, the SCAR is an electrical substitution radiometer operating at 20 K [23]. The detector of SCAR is a blackbody cavity with super high absorptance. Incident light induces a temperature increase in the blackbody cavity by absorption. The power of the incident light can be obtained by precisely measuring the electrical power applied in order to maintain constant temperature, as the incident light is duty cycled and its power is replaced by the electrical power. The heating effects of the incident light and electrical heater are nearly equivalent at 20 K, reducing non-equivalence corrections.

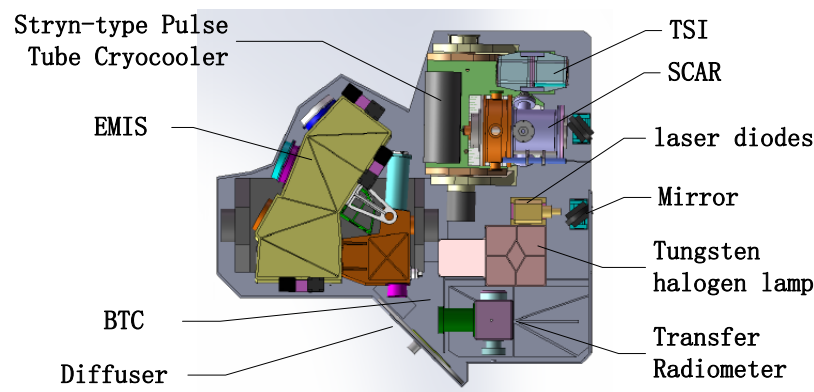


Figure 2. The design chart of Earth-Moon Imaging Spectrometer (EMIS) and Total Solar Irradiance (TSI).

Through the onboard calibration system, the radiometric scale of the reflected solar band and total solar irradiance can be traced to SCAR. The accuracy of the space cryogenic radiometric measurement, the in-orbit self-calibration, and the high spectral resolution radiance observation are the critical parts to the final performance of SCAR. The experimental prototype of SCAR has been in development since 2015. The Stryn-type Pulse Tube Cryocooler (SPTC) is used to obtain the 20 K working temperature. The SPTC is optimized to provide the refrigerating capacity of 350 mW at 20 K for space applications. The measurement uncertainty of the SCAR prototype is 0.029%, according to uncertainty analyses. The measurement uncertainty was verified by an indirect comparison with the ground-based cryogenic radiometer of the National Institute of Metrology (NIM) [24,25].

4.1.1. Earth-Moon Imaging Spectrometer

Reflected solar spectrum radiance is measured by the Earth-Moon Imaging Spectrometer (EMIS). The optical design of the EMIS consists of a telescope and a hyperspectral imaging spectrometer. The telescope utilizes a four-mirror anastigmat (4 MA) to eliminate aberrations. The hyperspectral imaging spectrometer is based on an Offner design. A prism is used as the dispersion element. The telescope uses the image space telecentric structure to achieve matching conditions with the pupil of the spectrometer, which uses a telecentric design. By setting baffles at the intermediate image plane, the influence of stray light is reduced. The EMIS makes a trade-off between the spectral and spatial resolution, with spectral and spatial sampling better than 10 nm and 100 m, respectively. The swath width is about 50 km at nadir from a 600 km orbit. The EMIS selects lens parameters, such as thickness, curvature, etc., to achieve lower dispersion non-linearities and better spectral performance.

The radiometric scale of the EMIS can be traced to SCAR. The measurement accuracy and long-term stability of the EMIS can be improved by the onboard hyperspectral calibration shown in Figure 3 and consists of the SCAR and Benchmark Transfer Chain (BTC). The SCAR will realize a long-term stable and highly accurate radiation measurement. The light power benchmark of SCAR is converted to a radiance benchmark by the Transfer Radiometer (TR) and multiple laser diodes. The multi-spectral calibration of the EMIS is realized by observing the reflected light of a diffuser. Based on the hyperspectral curve reconstruction technique, the EMIS is full-spectral calibrated by the TR and the tungsten halogen lamp inside an integrating sphere. In order to ascertain linearity over the large dynamic range, the Sun is used as the light source, with solar attenuations provided by attenuators.

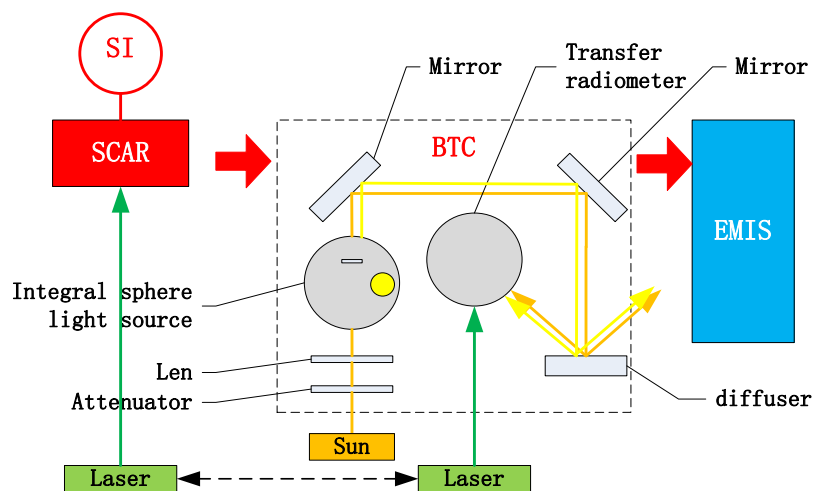


Figure 3. Schematic diagram of hyperspectral calibration on satellite.

4.1.2. Total Solar Irradiance

Total Solar Irradiance (TSI) is a kind of electrical substitution radiometer; the detector is alternately exposed to a radiant energy source (solar irradiance) and then, to known internal electrical heating. The temperature increase due to the absorbed solar irradiance is then compared to the same temperature increase due to a precisely measured equivalent electrical power. In order to improve the measurement uncertainty, the detector thermal compensation of TSI is investigated. The thermal conduction structure is optimized by the blackbody cavity design. Based on the application of a temperature bridge, the temperature drift of the heat sink is compensated to improve measurement repeatability.

The TSI calibration on the satellite is designed to improve the long-term stability of TSI measurements, as shown in Figure 4. The SCAR is also the benchmark of TSI calibration onboard the satellite. The SCAR and TSI are installed on the precision Sun tracker. The Sun Sensor (SS) is used to obtain the position of the Sun. Apertures suppress stray light in the TSI measurements. The irradiance scale of the TSI is traced to the SCAR via simultaneous solar observations. The system deviation is corrected by the real-time correction based on a super stable voltage reference. The TSI calibration on the satellite improves the absolute measurement accuracy and long-term stability.

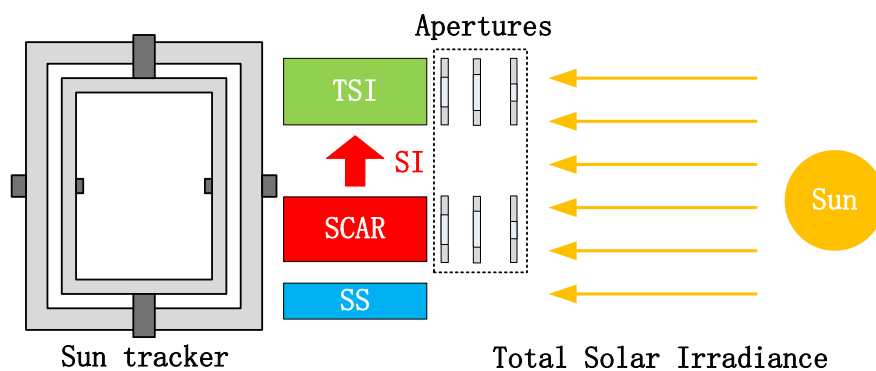


Figure 4. Schematic diagram of Total Solar Irradiance (TSI) calibration on satellite.

4.2. Solar Spectral Irradiance Traceable to Quantum Benchmark (SITQ)

We propose an approach to trace the solar spectral irradiance to Planck’s constant and photon count number by means of SPDC (Spontaneous Parametric Down-Conversion), a quantum optical effect occurring in a non-linear crystal pumped by a laser beam [26]. In an SPDC process, a one pump photon decays into a pair of photons, usually called correlated or entangled photons, since

they have definite relations between their frequencies, directions and polarizations. SPDC satisfies energy conservation $1/\lambda_p = 1/\lambda_1 + 1/\lambda_2$ and momentum conservation $k_p = k_1 + k_2$, where λ s are photon wavelengths, k s are wave vectors, and the subscript p , 1 and 2 denote pumping and correlated photons, respectively.

Detector calibration with SPDC is intrinsically absolute and independent of traceability to external radiometric standards. Theoretically, the accuracy of measured quantum efficiency is solely determined by how accurately the photon number is counted. This distinctive feature makes SPDC a promising candidate for an SI primary standard [27], as well as a space benchmark. With known quantum efficiency η , the photon detector can measure photon rate with $N = M/\eta$, or flux with $\Phi = Nh\nu$, or irradiance with $E = Nh\nu/A$, where A is the area of receiving aperture of the system. This forms the physical basis for tracing solar irradiance measurements to Planck's constant and the photon rate.

Figure 5 shows the concept of a solar spectral irradiance radiometer working in the visible to shortwave infrared spectrum and incorporating internal SPDC calibration. The radiometer has two working modes, i.e., a calibration mode for traceability to SI and an observation mode for solar irradiance measurement.

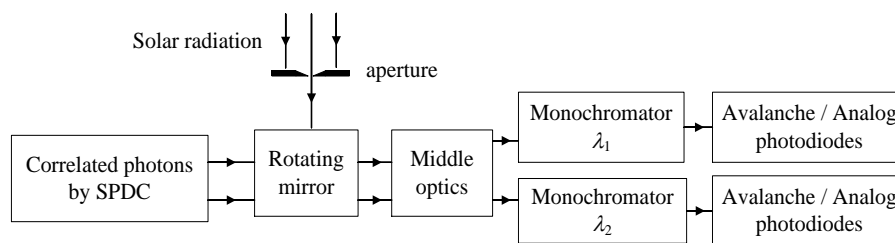


Figure 5. Concept for solar spectral irradiance measurement with Spontaneous Parametric Down-Conversion (SPDC) calibration.

In the calibration mode, correlated photons are directed by a rotating mirror into the middle optics, and then, are spectrally separated by two monochromators, before finally reaching avalanche photodiodes. The middle optics suppress residual pump photons and the monochromators ensure the wavelength correlation $1/\lambda_p = 1/\lambda_1 + 1/\lambda_2$. The calibration mode gives the quantum efficiency or absolute responsivity of the whole system and naturally accounts for any degradation of components of the system. This approach is especially useful as a reference or benchmark in space, and it appears advantageous over the endeavor to maintain a 'highly stable' onboard standard in space.

In the observation mode, solar radiation passes an entrance aperture and propagates along the same optical path before it is received by analogue photodiodes. The prototype uses analogue photodiodes, instead of single photon detectors, in the observation mode, since currently, no compact single photon detector is commercially available beyond 1700 nm, and solar photon rate is about five orders of magnitude higher than the maximum count rate of single photon detectors below 1700 nm under our current configuration. The absolute responsivities of the analogue photodiodes are determined in calibration mode by receiving a photon flux measured by avalanche photodiodes. Photon flux beyond 1700 nm is measured at their correlated wavelength below 1700 nm, given $N_1 = N_2$ at a pair of correlated wavelengths. The solar irradiance will be obtained as $E = Nh\nu/A$ with the known area A of entrance aperture.

4.3. IRS Based on Miniature Fixed-Temperature Phase-Change Cells

Aiming at a high precision traceability of measurements with the space reference for the infrared spectrum, an infrared sounder with hyperspectral resolution traceable to international units will be designed. Fourier infrared spectrum detection technology and miniature phase-change cells as temperature standard technology are adopted for the IRS. Schematic diagram of the optical system

for the IRS is drawn in Figure 6. Accurate blackbody temperatures (fixed points) are based on ‘phase-change cells’ technology.

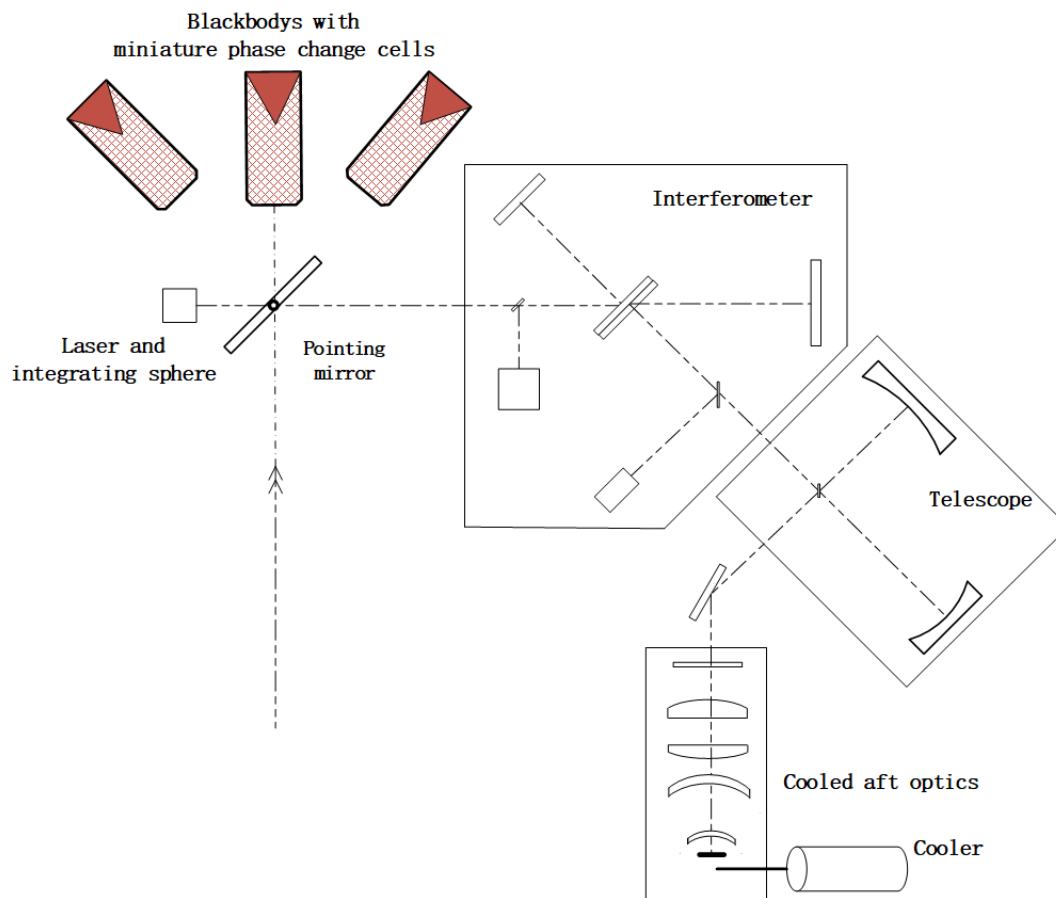


Figure 6. Schematic diagram of the optical system for the Infrared Spectrometer (IRS). Accurate blackbody temperatures (fixed points) are based on ‘phase-change cells’ technology.

Traceability chain of the IRS is shown in Figure 7. Three on-orbit absolute radiance IR calibrators realize on-orbit self-calibration of the cavity blackbody. An on-orbit temperature scale from 270 to 350 K is established using ITS-90 miniature phase-change cells traceable to ITS-90 with an uncertainty of better than 10 mK ($k = 2$) [28]. Based on high precision temperature control and a transfer method, the blackbody temperature is traceable to the SI standard. The blackbody emissivity is measured based on the controlled environment radiation method and is transferred to another blackbody using the laser.

The infrared interferometer realizes the high spectral resolution measurement over the infrared spectrum. The high sensitivity response over the wide spectral band is achieved by using a small-array detector. The high stability performance is realized by system temperature control technology using multiple temperature zones. High accuracy spectral calibration is achieved by referring to a standard spectral line source (high frequency infrared laser and gas absorption line).

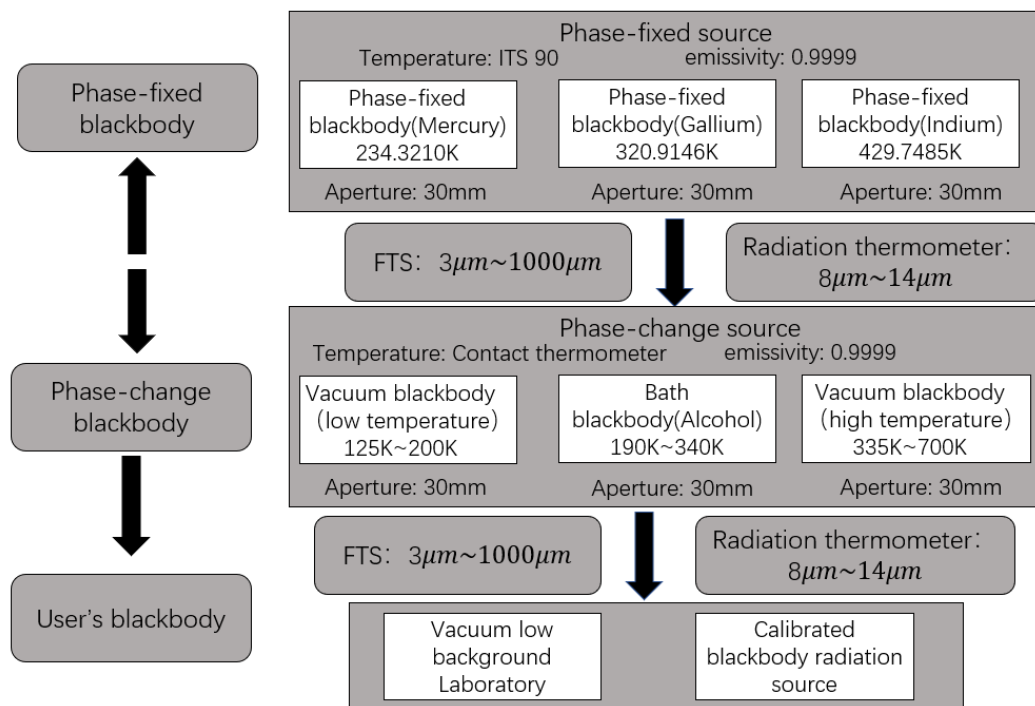


Figure 7. Traceability chain of the Infrared Spectrometer (IRS).

5. On-Orbit Mode to Support Intercalibration with Radiometric Traceability

In the calibration mode, LIBRA will be considered as the reference satellite to intercalibrate a target satellite with radiometric traceability. Intercalibration and the radiometric transfer from LIBRA to other satellites require the measurements from each spacecraft are taken along similar lines of sight, and within a few minutes of each other [29]. Similar techniques are currently used for intercalibration of satellite sensors within GSICS, an international effort to improve the consistency and accuracy of satellite intercalibration [12]. Examples of GSICS Products to support intercalibration with radiometric traceability are listed in Table 3. LIBRA would serve the international community by intercalibrating other Earth-observing instruments. The following sections describe the possible standard transfer methods from the LIBRA reference instruments.

Table 3. Products to support intercalibration with radiometric traceability.

Instruments	Products	Intercalibration Method	Example
IRS	Spectrally-resolved infrared radiance	Quasi-synchronous intercalibration	[16]
		LEO-LEO SNO	[30,31]
		GEO-LEO SNO	[32,33]
EMIS	Spectrally-resolved reflectance of solar radiation	Quasi-synchronous intercalibration	[34]
		LEO-LEO SNO	[35,36]
		GEO-LEO SNO	[37]
	Selected DCC reflectance	DCC	[38,39]
	Selected PICS reflectance	PICS	[40]
	Selected Lunar reflectance	Lunar	[41,42]

5.1. Quasi-Synchronous Intercalibration Transfer Mode by Orbital Maneuver

LIBRA will be operated such that its sub-satellite track is close to and overlaps with the track of the satellite to be intercalibrated (as seen in Figure 8). The intercalibration is carried out in near real-time in the nadir zone.

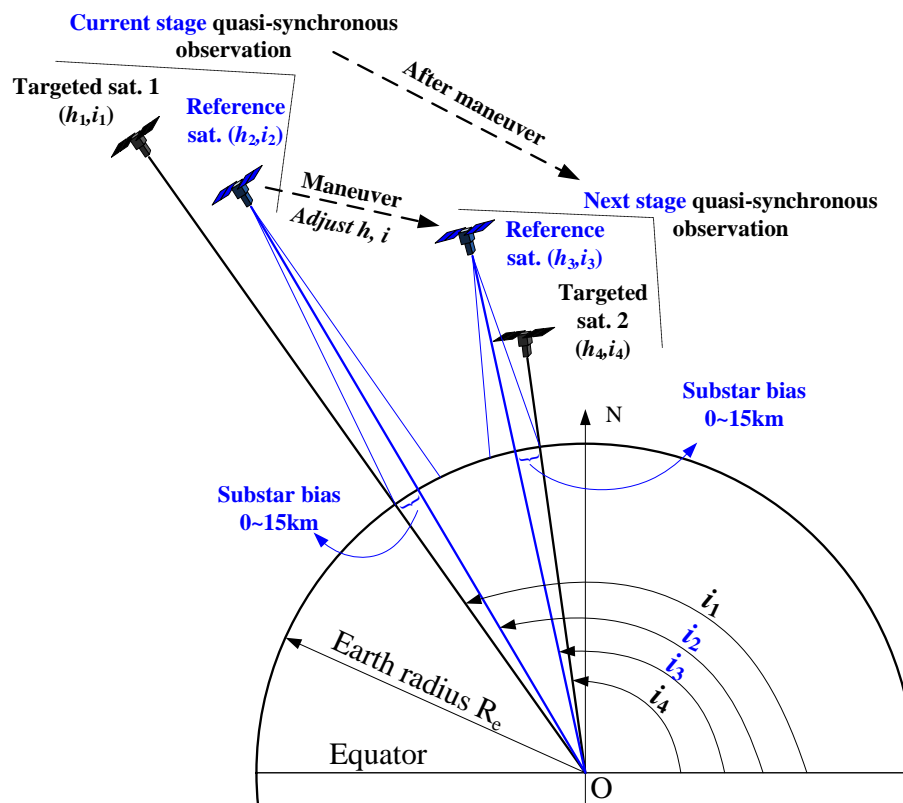


Figure 8. Quasi-synchronous intercalibration transfer mode by orbital maneuvers.

Calibration biases due to differences in viewing angles and sub-satellite tracks have to meet matching constraints between LIBRA and the target satellite to be calibrated. There is no need to carry out attitude maneuvers because collocated observations can be obtained over longer time periods.

In this mode, altitude and inclination adjustments for LIBRA are needed to conduct an intercalibration and to provide match-ups for intercalibration over a longer period. Because of the substantial fuel consumptions required to perform the orbit maneuvers, the quasi-synchronous mode will only be used when required by the target satellite. The frequency of such intercalibrations will depend on the available fuel of the satellite platform.

5.2. Simultaneous Nadir Overpass (SNO) Cross Intercalibration Transfer Mode (GEO-LEO or LEO-LEO)

With the reference satellite LIBRA and the targeted satellite flying in different orbital planes, the crossing area of the ground tracks is chosen as the intercalibration area. Differences in observation times and viewing angle have to meet certain requirements.

As depicted in Figure 9, LIBRA flies into the intercalibration area at time t_{C1} and point C1, and exits the area at time t_{C3} and point C3. When LIBRA observes within the intercalibration area, the attitude is adjusted such that LIBRA and the targeted satellite view the same area on the ground. The observation time differences $\Delta t = t_C - t_F$ shall be small enough to meet transfer accuracy requirements.

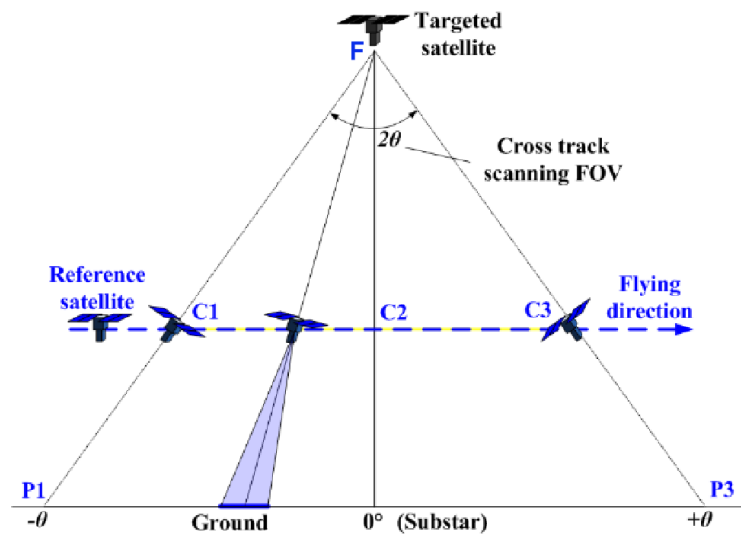


Figure 9. Simultaneous Nadir Observation (SNO) intercalibration transfer mode (Geostationary earth orbit (GEO)-Low earth orbit (LEO) or LEO-LEO).

5.3. Using Lunar Observations for Intercalibration

Observations of the Moon provide a viable method for the on-orbit cross calibration of Earth remote sensing instruments. Therefore, monthly lunar observations are major components of the on-orbit calibration strategies of LIBRA and other instruments. Taking the Moon as a calibration source, the reference and target satellite observe the same lunar phase which is realized by attitude maneuvers each month (as shown in Figure 10). Then, the intercalibration can be performed using a standard lunar radiation model, such as RObotic Lunar Observatory (ROLO) [43].

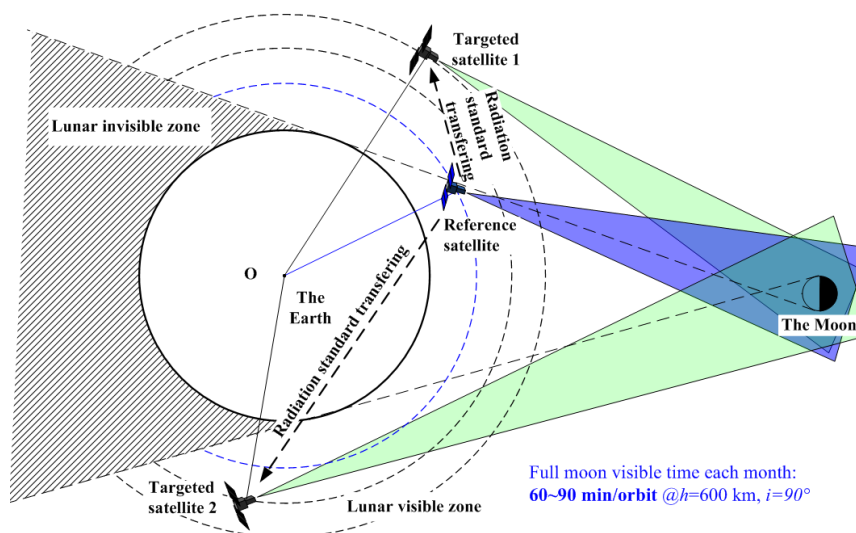


Figure 10. Lunar observation intercalibration transfer mode.

5.4. Using Vicarious Reference Targets for Intercalibration

The reference satellite can also observe stable targets such as Pseudo Invariant Calibration Sites (PICSs) and Deep Convective Clouds (DCC) over a long period of time, thereby collecting multiple angle observational data. Figure 11 shows the schematic diagram of intercalibration transfer mode using vicarious reference targets. When the target satellite flies over those reference sites or DCC, the co-located observations will be stored to monitor the long-term stability of instrument calibration [29].

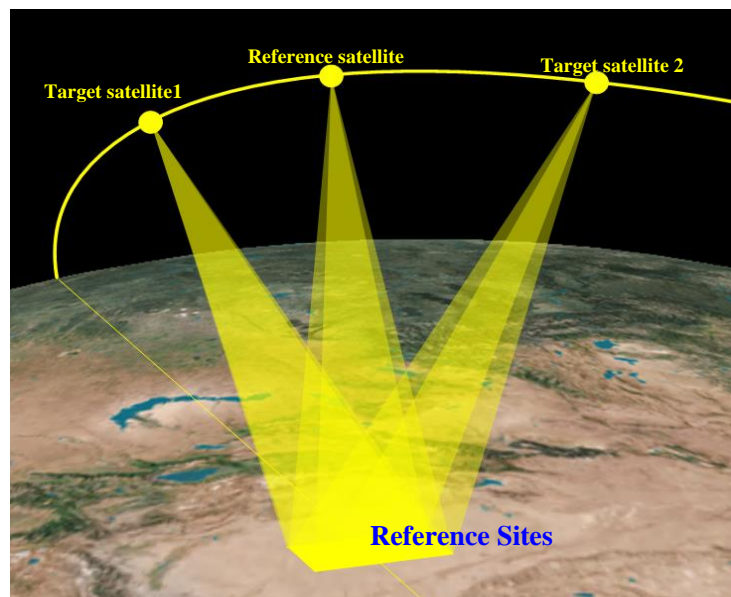


Figure 11. Intercalibration transfer mode using vicarious reference targets.

6. Balloon-Borne Demonstration System

When radiometric benchmark transfer methods are developed, an issue is the validation of the full chain of the space-based radiometric benchmark transfer. This problem is a primary motivation for the development of a balloon-borne demonstration system. There are three notable benefits in using this aerostat: First, the flight altitude of the aerostat can reach at least 18 km, above most of the atmosphere that contributes to the radiances observed from satellite. Second, there is a quasi-zero wind speed layer at the height range of 18–25 km in middle-latitude areas, such as over China, at the end of spring and in summer, so it is easier to have longer observations with the aerostat. Third, the onboard sensors can be recovered after a flight, so that high accuracy calibrations of sensors are feasible before and after an aerostat flight.

Considering the state of the art of aerostats, a high altitude balloon was chosen as the demonstration platform because it provides capacity for heavy payloads. However, the motion of the aerostat by the wind will affect spatial and temporal data matching between the aerostat and satellite. Therefore, before launching an aerostat flight mission, historical wind field data and the previous two days' radiosonde data will be collected to anticipate the balloon flight path, in order to choose the proper flight time and plan for an optimized flight path. During the flight, the flight control unit of the balloon can update the flight path, based on real-time wind fields, and precisely forecast the short-term trajectory and determine fall point of the payload cabin. Due to atmospheric friction, the payload cabin will rotate around the linkage cable. Therefore, azimuth of the payload is controlled with a flywheel alleviating balloon rotation. Precise calculation of sensor position and attitude will be realized through the onboard high accuracy position and orientation system (POS).

Currently, there are two reference sensors considered for the balloon test flights. The first is a simulator of the space-based benchmark spectroradiometer, covering a spectral range from 400 to 2500 nm with a spectral resolution of 3.5 nm@(400~1000 nm), 10 nm@(1000~1700 nm), 12 nm@(1700~2500 nm) and a maximum FOV of 10°. The second is a thermal sensor covering the same spectral range and a similar spectral resolution as the future space-based MIR-TIR benchmark sensor. Two blackbodies (BB), i.e., a high temperature (30 °C) BB and low temperature (10 °C) BB, are used to perform onboard calibration. The sensors are installed in a special chamber with high shock resistance and they are operated with active temperature control to maintain 20 °C.

At least two stratospheric balloon-based test flights will be performed in the demonstration phase. During each flight, there will be several flight phases of the aerostat: (i) launch, (ii) ascend,

(iii) observation, and (iv) descend (Figure 12). The total duration time is about 8 h, ensuring that there are at least 6 h for observations. Considering the narrow swath of balloon-based reference sensors, the balloon needs to observe uniform targets in order to alleviate influences of different resolutions of the to be calibrated satellite instruments. The Golmud area (94.9°E, 36.4°N) and Qinghai Lake (99.4°E, 36.3°N) are considered as candidate calibration sites. In the experiment, the Chinese high resolution GF series and the ZY series satellites, the FY series satellites, as well as Landsat-8, Sentinel-2, and NPP will be considered as satellites for which intercalibration will be demonstrated.

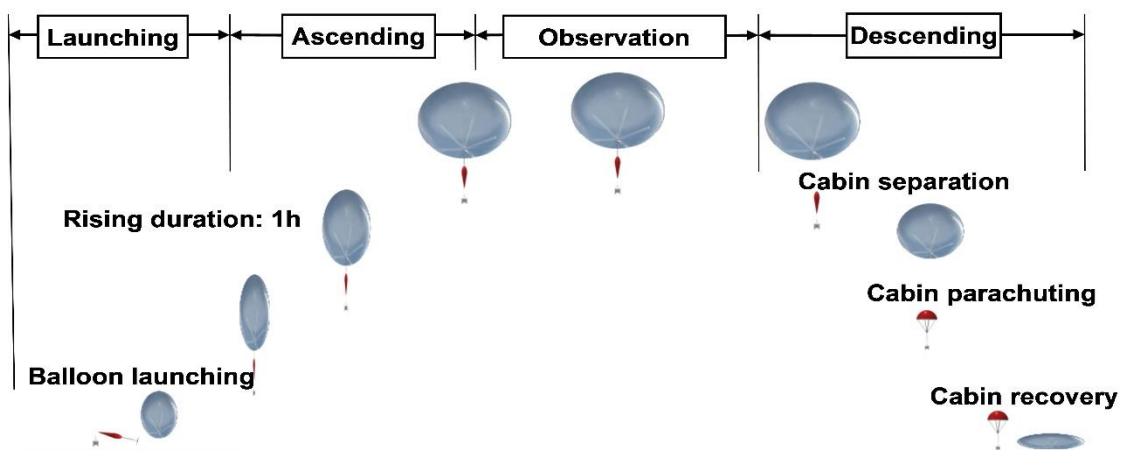


Figure 12. Sketch of flight test of the balloon-based demonstration system.

7. Conclusions

Accurate, long-term, consistent data are essential to climate science. Such data need to be calibrated to an absolute standard. The nature of satellite observations is the key to obtain global data of the earth and atmospheric system. However, so far, calibration directly traceable to a reference has not been possible for satellite observations. The principle of referring measurements to an absolute standard is not new, as it has been realized for in situ observations which are traceable to standards with well quantified uncertainties. This paper describes a novel space-based system, providing a similar traceability and accuracy for space-based radiance measurements. The realization of the LIBRA system will enable climate monitoring with much higher sensitivity to trend detection and provide benefits in science and economic terms [44].

LIBRA has important potential contributions to make to future climate observing systems, both directly through well-calibrated measurements and indirectly through facilitating intercalibration of the data from other platforms. LIBRA will measure solar reflected and infrared emitted high spectral resolution benchmark radiances, and provide accurate, credible, and tested climate records. These measurements will be used to detect climate change trends and test, validate, and improve climate prediction models. LIBRA can be used to calibrate other solar and infrared space-borne sensors and thereby improve climate monitoring accuracy for a wide range of measurements across the global space-based observing system.

As a complementary project to CLARREO and TRUTHS, LIBRA is expected to join an Earth observing satellite constellation and intends to contribute to space-based climate studies via publicly available data. Intercalibration of data from space-based observations falls under the auspices of the international CEOS Working Group on Calibration and Validation (WGCV) and GSICS. Therefore, intensive cooperation with the WGCV and GSICS is highly recommended during instrument development and data utilization of the LIBRA project.

Author Contributions: P.Z., N.L. and C.L. proposed the framework of the manuscript and supervised the progress. L.D., X.Z. (Xiaobing Zheng), X.Z. (Xuejun Zhang), X.H., X.Y., L.M. contributed to the designing of reference instruments, intercalibration modes, and Balloon-borne demonstration system. N.X., L.C., and J.S. aided in the manuscript revision. P.Z. prepared and finalised the manuscript. All authors contributed to the writing and commented on the manuscript. All authors have read and agreed to the published version of the manuscript.

Funding: This work has been supported by the National Key Research and Development Program of China (2018YFB0504900; 2018YFB0504800), and the Bureau of International Co-operation Chinese Academy of Sciences (181811KYSB20160040).

Acknowledgments: The authors do appreciate the discussion and comments from Kenneth Holmlund, Tim J. Hewison of EUMETSAT, Mitch Goldberg of NOAA, Nigel Fox of NPL, Bruce A. Wielicki of NASA, Greg Kopp of University of Colorado, and Wenjian Zhang of WMO. The authors are grateful to Wei Zhu and Wei Liang of Shanghai Institute of Satellite Engineering for their work concerning the orbit simulation and demonstration of Chinese LIBRA satellite.

Conflicts of Interest: The authors declare that they have no conflict of interest.

References

1. Dowell, M.; Lecomte, P.; Husband, R.; Schulz, J.; Mohr, T.; Tahara, Y.; Eckman, R.; Lindstrom, E.; Wooldridge, C.; Hilding, S.; et al. Strategy Towards an Architecture for Climate Monitoring from Space 2013. Available online: http://ceos.org/document_management/Working_Groups/WGClimate/Documents/ARCH_strategy-climate-architecture-space.pdf (accessed on 1 December 2019).
2. Global Climate Observing System (GCOS). *Systematic Observation Requirements for Satellite-Based Data Products for Climate, Supplemental Details to the Satellite-Based Component of the Implementation Plan for the Global Observing System for Climate in Support of the UNFCCC*; GCOS Report No. 154; GCOS: Geneva, Switzerland, 2011. Available online: <https://www.wmo.int/pages/prog/gcos/Publications/gcos-154.pdf> (accessed on 1 December 2019).
3. GCOS. *Status of the Global Observing System for Climate*; GCOS Report No. 195; GCOS: Geneva, Switzerland, 2015. Available online: <https://www.wmo.int/pages/prog/gcos/Publications/gcos-195.pdf> (accessed on 1 December 2019).
4. GCOS. *The Global Observing System for Climate: Implementation Needs*; GCOS Report No. 200; GCOS: Geneva, Switzerland, 2016. Available online: <https://www.wmo.int/pages/prog/gcos/Publications/gcos-200.pdf> (accessed on 1 December 2019).
5. *Climate Change 2014: Synthesis Report. Contribution of Working Groups I, II, and III to the Fifth Assessment Report of the Intergovernmental Panel on Climate Change*; Intergovernmental Panel on Climate Change (IPCC): Geneva, Switzerland, 2014.
6. Ohring, G.; Wielicki, B.; Spencer, R.; Emery, B.; Datla, R. Satellite instrument calibration for measuring global climate change—Report of a Workshop. *Bull. Am. Meteorol. Soc.* **2005**, *86*, 1303–1313. [[CrossRef](#)]
7. Hilton, F.; Armante, R.; August, T.; Barnet, C.; Bouchard, A.; Camy-Peyret, C.; Capelle, V.; Clarisse, L.; Clerbaux, C.; Coheur, P.-F.; et al. Hyperspectral Earth Observation from IASI: Five Years of Accomplishments. *Bull. Am. Meteorol. Soc.* **2012**, *93*, 347–370. [[CrossRef](#)]
8. Houghton, J.; Townshend, J.; Dawson, K.; Mason, P.; Zillman, J.W.; Simmons, A. The GCOS at 20 years: The origin, achievement and future development of the Global Climate Observing System. *Weather* **2012**, *67*, 227–235. [[CrossRef](#)]
9. Committee on Earth Observation Satellites (CEOS); Coordination Group for Meteorological Satellites (CGMS). Space Agency Response to GCOS Implementation Plan—The Joint CEOS/CGMS Working Group on Climate (WGClimate). ESA-ECO-EOPS-WGCL-RP-17-0061. 2017. Available online: http://ceos.org/document_management/Working_Groups/WGClimate/Documents/Space%20Agency%20Response%20to%20GCOS%20IP%20v2.2.1.pdf (accessed on 1 December 2019).
10. Fox, N.; Aiken, J.; Barnett, J.; Briottet, X.; Carvell, R.; Fröhlich, C.; Groom, S.; Hagolle, O.; Haigh, J.; Kieffer, H.; et al. Traceable radiometry underpinning terrestrial- and helio-studies (TRUTHS). *Adv. Space Res.* **2003**, *32*, 2253–2261. [[CrossRef](#)]
11. Wielicki, B.; Young, D.F.; Mlynczak, M.G.; Thome, K.J.; Leroy, S.; Corliss, J.; Anderson, J.G.; Ao, C.O.; Bantges, R.; Best, F.; et al. Achieving Climate Change Absolute Accuracy in Orbit. *Bull. Am. Meteorol. Soc.* **2013**, *94*, 1519–1539. [[CrossRef](#)]

12. Goldberg, M.; Ohring, G.; Butler, J.; Cao, C.; Datla, R.; Doelling, D.; Gärtner, V.; Hewison, T.; Iacovazzi, B.; Kurino, D.K.T.; et al. The Global Space-based Inter-calibration System. *Bull. Am. Meteorol. Soc.* **2011**, *92*, 467–475. [[CrossRef](#)]
13. World Meteorological Organization (WMO). Vision for the WMO Integrated Global Observing System in 2040. 2019. Available online: https://library.wmo.int/doc_num.php?explnum_id=10233 (accessed on 1 March 2020).
14. Bojinski, S.; Verstraete, M.; Peterson, T.C.; Richter, C.; Simmons, A.; Zemp, M. The Concept of Essential Climate Variables in Support of Climate Research, Applications, and Policy. *Bull. Am. Meteorol. Soc.* **2014**, *95*, 1431–1443. [[CrossRef](#)]
15. Gu, X.; Tong, X.D. Overview of China Earth Observation Satellite Programs. *IEEE Geosci. Remote Sens. Mag.* **2015**, *3*, 113–129.
16. Hu, X.; Zhang, Y.; Liu, Z.; Huang, Y.; Qiu, K.; Wang, Y.; Zhu, X.; Rong, Z. Optical characteristics of China Radiometric Calibration Site for Remote Sensing Satellite Sensors (CRCSRSS). In *Second International Asia-Pacific Symposium on Remote Sensing of the Atmosphere, Environment, and Space*; Society of Photo Optical: Bellingham, WA, USA, 2001; Volume 4151, pp. 77–86. [[CrossRef](#)]
17. Dong, C.; Yang, Z.; Lu, N.; Shi, J.; Zhang, W.; Yang, J.; Zhang, P.; Liu, Y.; Cai, B. An Overview of a New Chinese Weather Satellite FY-3A. *Bull. Am. Meteorol. Soc.* **2009**, *90*, 1531–1544. [[CrossRef](#)]
18. Datla, R.V.; Rice, J.; Lykke, K.; Johnson, B.C.; Butler, J.J.; Xiong, X. Best Practice Guidelines for Pre-Launch Characterization and Calibration of Instruments for Passive Optical Remote Sensing1. *J. Res. Natl. Inst. Stand. Technol.* **2011**, *116*, 621–646. [[CrossRef](#)] [[PubMed](#)]
19. Yang, J.; Zhang, P.; Lu, N.; Yang, Z.; Shi, J.; Dong, C. Improvements on global meteorological observations from the current Fengyun 3 satellites and beyond. *Int. J. Digit. Earth* **2012**, *5*, 251–265. [[CrossRef](#)]
20. Zhang, P.; Lu, Q.; Hu, X.; Gu, S.; Yang, L.; Min, M.; Chen, L.; Xu, N.; Sun, L.; Bai, W.; et al. Latest Progress of the Chinese Meteorological Satellite Program and Core Data Processing Technologies. *Adv. Atmos. Sci.* **2019**, *36*, 1027–1045. [[CrossRef](#)]
21. Lu, N.M.; Ding, L.; Zheng, X.B.; Ye, X.; Li, C.R.; Lu, D.R.; Zhang, P.; Hu, X.Q.; Zhou, C.H.; You, Z.; et al. Introduction of the radiometric benchmark satellite being developed in China for remote sensing. *J. Remote Sens.* **2020**, *24*, 672–680. (In Chinese)
22. Wang, Y.; Hu, X.; Wang, H.; Ye, X.; Fang, W. Standard transfer chain for radiometric calibration of optical sensing instruments with traceability in solar reflective bands. *Opt. Precis. Eng.* **2015**, *23*, 1807–1812. [[CrossRef](#)]
23. Xin, Y.; Xiaolong, Y.; Wei, F.; Kai, W.; Yang, L.; Zhiwei, X.; Yupeng, W.; Wang, Y.; Ye, X.; Yi, X.; et al. Design and investigation of absolute radiance calibration primary radiometer. *IET Sci. Meas. Technol.* **2018**, *12*, 994–1000. [[CrossRef](#)]
24. Yi, X.; Xia, Z.; Luo, Y.; Fang, W.; Wang, Y. Correction of cavity absorptance measure method for cryogenic radiometer. *IET Sci. Meas. Technol.* **2016**, *10*, 564–569. [[CrossRef](#)]
25. Yi, X.; Yang, Z.; Ye, X.; Wang, K.; Fang, W.; Wang, Y.P. Absorptance measurement for sloping bottom cavity of cryogenic radiometer. *Opt. Precis. Eng.* **2015**, *23*, 2733–2739. [[CrossRef](#)]
26. Louisell, W.H.; Yariv, A.; Seigman, A.E. Quantum Fluctuations and Noise in Parametric Processes. *Phys. Rev.* **1961**, *124*, 1646–1654. [[CrossRef](#)]
27. Lemieux, S.; Giese, E.; Fickler, R.; Chekhova, M.V.; Boyd, R.W. A primary radiation standard based on quantum nonlinear optics. *Nat. Phys.* **2019**, *15*, 529–532. [[CrossRef](#)]
28. Hao, X.P.; Sun, J.P.; Xu, C.Y.; Wen, P.; Song, J.; Xu, M.; Gong, L.Y.; Ding, L.; Liu, Z.L. Miniature Fixed Points as Temperature Standards for In Situ Calibration of Temperature Sensors. *Int. J. Thermophys.* **2017**, *38*, 90. [[CrossRef](#)]
29. Chander, G.; Hewison, T.J.; Fox, N.; Wu, X.; Xiong, X.; Blackwell, W.J. Overview of Intercalibration of Satellite Instruments. *IEEE Trans. Geosci. Remote Sens.* **2013**, *51*, 1056–1080. [[CrossRef](#)]
30. Cao, C.; Xu, H.; Sullivan, J.; McMillin, L.; Ciren, P.; Hou, Y.-T. Intersatellite Radiance Biases for the High-Resolution Infrared Radiation Sounders (HIRS) on board NOAA-15, -16, and -17 from Simultaneous Nadir Observations. *J. Atmos. Ocean. Technol.* **2005**, *22*, 381–395. [[CrossRef](#)]
31. Wu, C.; Qi, C.; Hu, X.; Gu, M.; Yang, T.; Xu, H.; Lee, L.; Yang, Z.; Zhang, P. FY-3D HIRAS Radiometric Calibration and Accuracy Assessment. *IEEE Trans. Geosci. Remote Sens.* **2020**, *58*, 3965–3976. [[CrossRef](#)]

32. Gunshor, M.M.; Schmit, T.; Menzel, W.P.; Tobin, D.C. Intercalibration of Broadband Geostationary Imagers Using AIRS. *J. Atmos. Ocean. Technol.* **2009**, *26*, 746–758. [[CrossRef](#)]
33. Hu, X.; Xu, N.; Weng, F.; Zhang, Y.; Chen, L.; Zhang, P. Long-Term Monitoring and Correction of FY-2 Infrared Channel Calibration Using AIRS and IASI. *IEEE Trans. Geosci. Remote Sens.* **2013**, *51*, 5008–5018. [[CrossRef](#)]
34. Minnis, P.; Doelling, D.R.; Nguyen, L.; Miller, W.F.; Chakrapani, V. Assessment of the Visible Channel Calibrations of the VIRS on TRMM and MODIS on Aqua and Terra. *J. Atmos. Ocean. Technol.* **2008**, *25*, 385–400. [[CrossRef](#)]
35. Cao, C.; Weinreb, M.; Xu, H. Predicting Simultaneous Nadir Overpasses among Polar-Orbiting Meteorological Satellites for the Intersatellite Calibration of Radiometers. *J. Atmos. Ocean. Technol.* **2004**, *21*, 537–542. [[CrossRef](#)]
36. Heidinger, A.; Cao, C.; Sullivan, J.T. Using Moderate Resolution Imaging Spectrometer (MODIS) to calibrate advanced very high resolution radiometer reflectance channels. *J. Geophys. Res. Space Phys.* **2002**, *107*, AAC-11. [[CrossRef](#)]
37. Minnis, P.; Nguyen, L.; Doelling, D.; Young, D.F.; Miller, W.F.; Kratz, D.P. Rapid Calibration of Operational and Research Meteorological Satellite Imagers. Part I: Evaluation of Research Satellite Visible Channels as References. *J. Atmos. Ocean. Technol.* **2002**, *19*, 1233–1249. [[CrossRef](#)]
38. Fougnie, B.; Bach, R. Monitoring of Radiometric Sensitivity Changes of Space Sensors Using Deep Convective Clouds: Operational Application to PARASOL. *IEEE Trans. Geosci. Remote Sens.* **2008**, *47*, 851–861. [[CrossRef](#)]
39. Chen, L.; Hu, X.; Xu, N.; Zhang, P. The Application of Deep Convective Clouds in the Calibration and Response Monitoring of the Reflective Solar Bands of FY-3A/MERSI (Medium Resolution Spectral Imager). *Remote Sens.* **2013**, *5*, 6958–6975. [[CrossRef](#)]
40. Chander, G.; Xiong, X.; Choi, T.; Angal, A. Monitoring on-orbit calibration stability of the Terra MODIS and Landsat 7 ETM+ sensors using pseudo-invariant test sites. *Remote Sens. Environ.* **2010**, *114*, 925–939. [[CrossRef](#)]
41. Stone, T.C.; Rossow, W.B.; Ferrier, J.; Hinkelman, L.M. Evaluation of ISCCP multi-satellite radiance calibration for geostationary imager visible channels using the moon. *IEEE Trans. Geosci. Remote Sens.* **2013**, *51*, 1255–1266. [[CrossRef](#)]
42. Zhang, L.; Zhang, P.; Hu, X.; Chen, L.; Min, M.; Xu, N.; Wu, R. Radiometric Cross-Calibration for Multiple Sensors with the Moon as an Intermediate Reference. *J. Meteorol. Res.* **2019**, *33*, 925–933. [[CrossRef](#)]
43. Kieffer, H.H.; Stone, T.C. The Spectral Irradiance of the Moon. *Astron. J.* **2005**, *129*, 2887–2901. [[CrossRef](#)]
44. Cooke, R.M.; Wielicki, B.A.; Young, D.F.; Mlynczak, M. Value of information for climate observing systems. *Environ. Syst. Decis.* **2013**, *34*, 98–109. [[CrossRef](#)]



© 2020 by the authors. Licensee MDPI, Basel, Switzerland. This article is an open access article distributed under the terms and conditions of the Creative Commons Attribution (CC BY) license (<http://creativecommons.org/licenses/by/4.0/>).